Available online at www.sciencedirect.com
ScienceDirect
Powder Technology 173 (2007) 38–50
POWDER TECHNOLOGY
www.elsevier.com/locate/powtec

Analysis of four Monte Carlo methods for the solution of population balances in dispersed systems

H. Zhao [a], A. Maisels [b], T. Matsoukas [c,*], C. Zheng [a]

[a] State Key Laboratory of Coal Combustion, Huazhong University of Science andTechnology, Wuhan, 430074 Hubei, PR China
[b] Process Technology, Degussa AG, Hanau-Wolfgang, D-63457, Germany
[c] 150 Fenske Laboratory, Department of Chemical Engineering, Pennsylvania State University, PA 16802, United States

Received 8 September 2006; received in revised form 13 November 2006; accepted 5 December 2006
Available online 8 December 2006

Abstract

Monte Carlo (MC) constitutes an important class of methods for the numerical solution of the general dynamic equation (GDE) in particulate systems. We compare four such methods in a series of seven test cases that cover typical particulate mechanisms. The four MC methods studied are: time-driven direct simulation Monte Carlo (DSMC), stepwise constant-volume Monte Carlo, constant number Monte Carlo, and multi-Monte Carlo (MMC) method. These MC's are introduced briefly and applied numerically to simulate pure coagulation, breakage, condensation/evaporation (surface growth/dissolution), nucleation, and settling (deposition). We find that when run with comparable number of particles, all methods compute the size distribution within comparable levels of error. Because each method uses different approaches for advancing time, a wider margin of error is observed in the time evolution of the number and mass concentration, with event-driven methods generally providing better accuracy than time-driven methods. The computational cost depends on algorithmic details but generally, event-driven methods perform faster than time-driven methods. Overall, very good accuracy can be achieved using reasonably small numbers of simulation particles, $O(10^3)$, requiring computational times of the order 10^2–10^3 s on a typical desktop computer.

Keywords: Population balance; Monte Carlo; Coagulation; Breakup; Nucleation

1. Introduction

Dynamic phenomena in dispersed systems, such as particle birth (nucleation etc.), death (settling, or saying, deposition), size enlargement (coagulation, surface growth, etc.), and disintegration (breakage, surface dissolution, etc.) are of great importance for both natural and laboratory systems. Indeed, these processes are inherent for aerosols, particulate matter, colloidal suspensions, nanoparticles, emulsions, polymers, galaxies, etc. For example, trace metal enrichment on particulate matter (PM) for pulverized-coal-fired power plants is dominated by condensation, coagulation and nucleation [1]; both coagulation and breakage, take place simultaneously during long chain polymer synthesis in chemical engineering, leading to an equilibrium distribution [2]; PM inside a turbulent exhaust plume of a diesel engine is formed by a number of processes including homogeneous nucleation and coagulation [3]. The particle size distribution (PSD) usually evolves in both time and space under the influence of these dynamic events. Since many important properties of dispersed particles, such as light scattering, electrostatic charging, toxicity, radioactivity, sedimentation, capturing strategy, etc, depend on their size distribution, the time evolution of size distribution is issue of fundamental interest.

The evolution of the particle size distribution is mathematically represented by the population balance equation (PBE). In the presence of coagulation, breakage, nucleation, surface

* Corresponding author.
E-mail addresses: klinsmannzhb@163.com (H. Zhao), arkadi.maisels@degussa.com (A. Maisels), matsoukas@psu.edu (T. Matsoukas).

0032-5910/$ - see front matter © 2006 Elsevier B.V. All rights reserved.
doi:10.1016/j.powtec.2006.12.010

growth/dissolution (condensation/evaporation) and settling (deposition) this equation is as follows:

$$\frac{\partial n(v)}{\partial t} = \underbrace{\frac{1}{2}\int_0^v \beta(v-u,u)n(v-u)n(u)du - \int_0^\infty \beta(v,u)n(v)n(u)du}_{\text{coagulation}} + \underbrace{\int_0^v \Gamma(v|u)S(u)n(u)du - S(v)n(v)}_{\text{breakage}} + \underbrace{J(v)\delta(v_{\text{nuc}},v)}_{\text{nucleation}} + \underbrace{C_S K_S(v-v_S)n(v-v_S) - C_S K_S(v)n(v)}_{\text{surface growth/dissolution}} + \underbrace{-E(v)n(v)}_{\text{settling}} + \underbrace{+\cdots}_{\text{other}} \quad (1)$$

Here, v is the particle volume (m^3), taken to represent size; $n(v)$(m^{-6}) is the size distribution such that $n(v)dv$ (m^{-3}) is the number concentration of particles in the size range v to $v+dv$; $\beta(v,u)$is the coagulation rate constant between sizes v and u (m^3/s); $S(v)$ (s^{-1}) is the breakage rate of size v; $\Gamma(v|u)$ (m^{-3}) is the number concentration of fragments of size v to $v+dv$ produced by the breakage of size u; J (v)(m^{-6} s^{-1}) is the nucleation rate; v_{nuc} (m^3) is the size of the nucleus; C_S (m^{-3}) is the concentration of the condensing species; $K_S(v)$ (m^3/s) is the rate of surface deposition onto particles of size v; v_S (m^3) is the volume of the condensing species; and $E(v)$ (s^{-1}) is the rate of loss of particles with size v by settling or other mechanisms.

This equation can, in principle, be solved once the initial conditions and all rate laws are specified. In practice, this is a complex task due to the integro-differential nature of the equation which requires discretization in both time and size. The methodologies available for its solution can be divided into deterministic and stochastic. On the deterministic front, the possible choices include the method of moments [4–15], sectional method [16], discrete method [17] and discrete-sectional method [18,19]. In these methods the required integrals are calculated either through an appropriate discretization scheme, or by quadrature. In contrast to deterministic integration, stochastic methods utilize Monte Carlo (MC) to simulate the evolution of a finite sample of the particle population [20–36].

The discrete nature of MC method, which is based on the physical model of dispersed systems, adapts itself naturally to dynamic process. Population balance problems and MC methods are integrated seamlessly into a single framework as they both have deal with discrete events. Several applications of MC to population balances have appeared in recent years, including agglomeration [37], coalescence [20,38], restructuring [39,40], higher-dimensionality problems [41], multi-component aerosols [42], coating [31], chemical reaction [43], crystallization [44], bipolar charging [45], fractal aggregation [46] and wet scavenging [33]. In MC-based methods, discretization of the size distribution is not required. This simplifies the programming effort significantly compared to deterministic methods and allows the inclusion of multiple mechanisms (coagulation, breakup, etc.) in a straightforward manner. The simultaneous solution of population balances and the Navier–Stokes equations is also possible if fluid mechanics are treated in a stochastic manner [47]. With regards to multicomponent — and multivariate, in general — problems, Monte Carlo essentially represents the only practical choice for obtaining distributions that depends on more than one size coordinate [48]. At present, the main disadvantage of MC methods is that they cannot be easily interfaced with standard process simulators, which generally implement deterministic integration routines.

MC methods can be divided into two classes according to the treatment of the time step. These are referred to as "time-driven" and "event-driven" MC. In time-driven simulations a time step is specified, then the simulation implements all possible events within that step [23]. In event-driven, first an event is implemented, then the time is advanced by an appropriate amount [22]. Monte Carlo methods can be further classified according to whether or not the total number of simulation particles is changed during the course simulation. In the classical approach [22], the simulation tracks a constant reaction volume in which the number of particles varies depending on the mechanisms that transform the particle distribution. For example, in coagulation the number of particles decreases continuously while in fragmentation it increases. A practical difficulty with this implementation is that prolonged simulation causes the number of particles to exceed the bounds of the simulation box, as when coagulation reduces the number of particles to one, or when fragmentation produces more particles than the size of the simulation box. This problem can be avoided by "regulating" the number of particles, periodically or continuously, so as to maintain the number of simulated particles within bounds [23,24,31]. These features may be combined to construct Monte Carlo variants that implement event- or time-driven MC with regulated or variable number of simulation particles. This has created a situation in which the potential user is left with no firm basis for selecting the most suitable method for a given problem. Limited comparisons have appeared in the literature [32], however, a comprehensive study of different Monte Carlo methods on a wide range of problems is lacking. The purpose of this paper is to provide such comparison and to develop criteria that may guide the user through the selection of the appropriate techniques. To this end, we test four algorithms and their variations over a common set of problems that include coagulation, breakup, condensation/evaporation (surface growth/dissolution), nucleation and settling (deposition). The four methods studied are:

- Constant number MC: this is an event-driven method in which the number of particles remains constant and equal to a value specified at the beginning of the simulation [24–26].
- Stepwise constant-volume MC: this method is also event-driven and regulates the number of particles periodically in order to keep them within the bounds of the simulation box [31,32].
- Direct simulation Monte Carlo developed by Liffman [23] (noted as time-driven DSMC). This is a time-driven simulation with periodic regulation of the number of particles.
- Multi-Monte Carlo: This method is time-driven and combines elements of constant-number and constant-volume Monte Carlo [33–36].

These methods are described in the next section.

2. Introduction of four MC methods

2.1. Constant-number MC

The constant number method [24–26] is an event-driven simulation. In the context of population balances, "event" refers to a specific action (transformation) involving particles, for example, aggregation of particles i and j, breakup of particle k, surface deposition onto particle l, etc. At each step of the simulation, a single event is implemented, the size of the simulation box is adjusted and the time increment is computed. The special feature of this method is the restoration of the simulation box to the desired size, which is done as explained below. In coagulation, each event removes a particle from the simulation box. This vacancy is filled by randomly choosing a particle in the simulation box and placing its copy in the simulation box. In k-nary fragmentation, each event produces a net $k-1$ fragments that must be accommodated. In this case, $k-1$ randomly selected particles in the simulation box are erased. This approach ensures that the number of particles in the simulation box after each event is the same as before the event, regardless of whether the particle concentration increases or decreases with time. The continuous regulation of the simulation size requires special treatment of the time increment and of the mass and number concentrations of the particles [26]. The mass concentration, V, of the particles is computed from the difference equation

$$\frac{\Delta V}{V} = \frac{\delta v_{\text{event}}}{N\overline{v}} \tag{2}$$

in which, N is the constant number of particles in the simulation box, $\overline{v}$ is the mean size (mass) in the box, and δv_{event} is the change (positive, negative, or zero) in the mass of the system as a result of the event implemented. In coagulation and fragmentation, $\delta v_{\text{event}}=0$, since mass is conserved for these processes; in nucleation it is positive and equal to the mass of the nucleus, v_{nuc}; in evaporation it is negative and equal to $-v_S$, where v_S is the mass of the evaporating species. The number concentration, C is calculated from the mass concentration and the known average size,

$$C = \frac{V}{\overline{v}} \tag{3}$$

and the time increment is given by [26]

$$\Delta t = \frac{C}{N}\frac{1}{\sum_i R_i} \tag{4}$$

where $\sum_i R_i$ the sum of the rate per unit volume ($m^{-3}\ s^{-1}$) of all processes that take place. Eqs. (2) and (3) are based on the requirement that the mass concentration of particles must remain the same before and after restoration. It is possible to derive an alternative set of equations by enforcing a similar requirement for the number concentration. Lin et al. [26] have shown that this approach is less accurate, therefore, it is not considered in the present study.

2.2. Stepwise constant-volume method

This is an event-driven method that operates in constant-volume mode but which periodically adjusts the number of particles in the simulation box. During the constant-volume part, the simulation box contains N particles, whose number varies according to the particulate event that is implemented in each step. The number concentration that corresponds to the number of particles in the box is

$$C = \frac{N}{N_0}C_0 \tag{5}$$

where C_0 is the particle concentration at time zero and N_0 is the initial number of particles in the simulation box. The mass concentration is $V=Cv$ and the time increment is obtained from

$$\Delta t = \frac{C_0}{N_0}\frac{1}{\sum_i R_i} \tag{6}$$

The number of particles is regulated periodically following a procedure used by Liffman [23] and extended by Maisels et al. [32]: if the number of particles during simulation increases, it is halved once it reaches the value $2N_0$; if the number in the simulation box decreases, then it is doubled when it reaches $N_0/2$. With each doubling or halving of the simulation box, the right-hand sides of Eqs. (5) and (6) must be multiplied with $2^{\pm 1}$ (with the − sign for doubling and the + sign for halving) to ensure that concentrations and time are not affected by the change in the simulation box. We also note that in the case of coagulation, the doubling of the sample creates a new sample with identical statistics, thus avoiding the noise introduced by the random selection of the particles to fill the box, as done in constant − N MC.

2.2.1. Selection of events

Event-driven methods require the selection of an event at each time step. This is done in a two-step fashion. First, it is decided which process (coagulation, fragmentation, etc.) is to take place. This decision is made with a probability P_i, given by

$$P_i = \frac{R_i}{\sum_l R_l} \tag{7}$$

where R_l is the rate per unit volume ($m^{-3}s^{-1}$) of each process (l=coagulation, fragmentation, etc.) and $\sum R_l$ the sum of all rates. Expressions for the probability of the various processes considered in this study are summarized in Table 1. Once a process has been chosen, the simulation must choose a specific particle or particle pair that must undergo the transformation specified by the process. Two common methods by which this may be accomplished are the acceptance/rejection method, and the so-called inverse (or cumulative probability) method. Both are briefly explained below, using coagulation as an example. In the acceptance/rejection method, a pair of particles, (i,j), is selected at random and is accepted for coagulation with probability

$$P_{ij} = \frac{\beta(v_i, v_j)}{\sum_i \sum_{j\neq i} \beta(v_i, v_j)} \tag{8}$$

Table 1
Time steps and probabilities for different dynamic processes

Event l	$t_{i,l}$ (time-driven DSMC)	$t_{i,l}$ (MMC)	R_l
Coagulation	$\frac{V_s}{\sum_{j\neq i}\beta_{ij}}$	$\frac{V_s}{\sum_{j\neq i}k_{wt,i}\beta_{ij}}$	$\frac{1}{2V_s^2}\sum_i\sum_{j\neq i}\beta_{ij}$
Breakage	$\frac{1}{S_i}$	$\frac{1}{S_i}$	$\frac{1}{V_s}\sum_i S_i$
Surface growth	$\frac{1}{C_S K_S(v_i)}$	$\frac{1}{C_S K_S(v_i)}$	$\frac{C_S}{V_S}\sum_i K_S(v_i)$
Nucleation	$\frac{1}{V_s^2 J(v)\delta(v_{nuc}, v)}$	$\frac{1}{V_s^2 J(v)\delta(v_{nuc}, v)}$	$V_s J(v)\delta(v_{nuc}, v)$
Settling	$\frac{1}{E_i}$	$\frac{1}{E_i}$	$\frac{1}{V_s}\sum_i E_i$

R_l is the rate per unit volume of event l (m^{-3} s^{-1}).
V_s is the volume of the simulated system (m^3).

in which the numerator is the coagulation kernel for the selected particles and the denominator is the normalizing factor. The pair is accepted if the condition, rnd $\leq P_{ij}$, is met, where rnd is a random number from a uniform distribution in the interval [0, 1]. If the condition is not met, the pair is rejected and the process is repeated until the acceptance condition is met. The method is simple to program but suffers from high rejection rates for certain types of kernels. The acceptance ratio can be improved if the denominator in Eq. (8) is replaced by the maximum term of the summation. This increases the absolute value of P_{ij} while ensuring that is less than unity. This substitution results in additional savings in computational time as the double summation in the denominator of Eq. (8) is not required.

The inverse method avoids the problem of rejections by always accepting the selected pair. This is done by constructing the cumulative distribution of P_{ij} from Eq. (8) (see for example Ref. [22]). A random number rnd in the interval [0, 1] is drawn and the double summation $\sum_{i=1}^{N}\sum_{j=i+1}^{N} P_{ij}$ is built sequentially, until the condition

$$\sum_{i=1}^{i'}\sum_{=i+1}^{j'} P_{ij} \leq \text{rnd} \tag{9}$$

is violated for some pair (i', j'). The last pair (i, j) to satisfy this condition is the one selected to coagulate. While no time is wasted in rejections, the inverse method requires the computation of the double summations in Eqs. (8) and (9) after each event and demands overall more programming effort compared to the acceptance/rejection.

2.3. Time-driven direct simulation MC (DSMC) with particle regulation

This method was described by Liffman [23] for coagulation and has been extended here to include other particulate mechanisms. This MC belongs to time-driven methods and uses a periodic regulation of the number of particles in the simulation box. In time-driven MC, the time increment, Δt, is fixed, and every simulation particle is tracked to determine whether it participates in an event within that time interval. For example, particle i undergoes coagulation if the following condition is met:

$$\text{rnd} < 1 - \exp[-\Delta t / 2t_{\text{coag},i}] \tag{10}$$

where

$$t_{\text{coag},i} = \frac{V_s}{\sum_j \beta(v_i, v_j)} \tag{11}$$

is the mean coagulation time of particle i, V_s is the volume of the simulated system, and rnd is a random number in the interval [0, 1]. The coagulation partner of particle i, particle j, is determined with probability

$$P'_{ij} = \frac{\beta(v_i, v_j)}{\sum_j \beta(v_i, v_j)} \tag{12}$$

using the method of cumulative probabilities. The time increment, Δt, is computed as

$$\Delta t = \alpha \min_i \{t_{\text{coag},i}\} \tag{13}$$

where α is a small multiplicative constant, typically $\alpha \leq 0.01$. By setting the time increment to an interval smaller than the fastest process in the simulation ensures that at most one event occurs within time Δt. The precise choice of the parameter α requires some trial so as to improve the accuracy of the calculation. The number of particles in the simulation box is regulated by periodic doubling or halving, using the same procedure of the stepwise constant-volume method.

2.4. Multi-Monte Carlo (MMC)

This Monte Carlo method belongs to the time-driven variant. The main departure in this algorithm is the use of a statistical weight, k_{wt}, that characterizes each simulation particle. In all of the methods discussed so far, a particle in the simulation box can be thought to represent C/N particles in the real system, where N is the number of particles in the simulation box, and C is the number of particles in the real system. This scale factor is the same for all particles in the simulation box. In the MMC method, a simulation particle is viewed to represent a group of particles with a weight factor k_{wt} that represents the number of real particles in that group [33–36]. The MMC method is based on time-driven MC technique, the main idea of which is similar to time-driven DSMC except that the simulation also tracks the weight factors, k_{wt}.

The method is briefly outlined here using breakage as an example. First, the time step, Δt is set as in Eq. (13) based on the fastest breakup time in the system. Breakage of particle i is implemented if the condition

$$\text{rnd} < S(v_i)\Delta t \tag{14}$$

is met, where rnd is a random number in the interval [0,1]. Upon fragmentation, all fragments inherit the weight factor of the parent particle. To regulate the number of particles, one fragment is stored in the position of the parent particle and all others are merged with simulation particles whose mass most closely matches that of the fragment; if more than one such simulation particles match the mass of the fragment, one is chosen randomly. Suppose, for example, that particle i generates fragments i_1 and i_2. The first fragment replaces the parent particle while the second fragment replaces a particle j whose mass closely matches v_{i_2}. The masses and weight factors of the particles that now occupy the positions i and j are computed as follows:

$$\begin{array}{ll} (v_i)_{\text{new}} = v_{i_1}; & (k_{\text{wt},i})_{\text{new}} = k_{\text{wt},i} \\ (v_j)_{\text{new}} = (v_j)_{\text{old}}; & (k_{\text{wt},j})_{\text{new}} = (k_{\text{wt},j})_{\text{old}} + k_{\text{wt},i} \end{array} \quad (15)$$

The first equation replaces the mass of particle i with the mass of the first fragment; the second equation increases the weight factor of particle j by that of the second fragment. In this method, the number of simulation particles remains constant while concentrations are tracked via the weight factors of the particles.

3. Results

3.1. The test cases

The four methods are applied to a set of standard problems involving coagulation, breakage, surface deposition (condensation), nucleation, and settling. These represent a wide range of particulate mechanisms and result in population balance equations whose right-hand side ranges from integral form, to differential, to algebraic. The seven cases examined in this paper are summarized below:

Case 1. Coagulation with size-independent coagulation kernel,

$$\beta(v_i, v_j) = \beta_0 = 10^{-10}\text{m}^3\text{s}^{-1} \quad (16)$$

and with initial particle concentration $C_0 = 10^{10}$ m^{-3}.

Case 2. Coagulation with linear kernel,

$$\beta(v_i, v_j) = \beta_0 \frac{v_i + v_j}{v_0} \quad (17)$$

with $\beta_0 = 10^{-10}$ m^3 s^{-1} and initial particle concentration $C_0 = 10^{10}$ m^{-3}.

Case 3. Coagulation with quadratic kernel,

$$\beta(v_i, v_j) = \beta_0 \frac{v_j v_j}{v_0^2} \quad (18)$$

with $\beta_0 = 10^{-10}$ m^3 s^{-1} and initial particle concentration $C_0 = 10^{10}$ m^{-3}.

Case 4. Breakage into 12 equal-size fragments with power-law breakage rate,

$$S(v) = S_0 \left(\frac{v}{v_0}\right)^{1.8}, \quad S_0 = 1\ s^{-1} \quad (19)$$

and with initial particle concentration of 3×10^3 m^{-3}.

Case 5. Surface growth. In this model, a chemical precursor with dimensionless size $v_s/v_0 = 1$ deposits onto the surface of seed particles with a growth rate that has linear dependence on the size of the particle, $K_S(v) = 10^{-10} v$ (m^3 s^{-1}). The initial concentration of the precursor molecules is 10^{10} m^{-3} and the concentration of seed particles is $C_0 = 10^{10}$ m^{-3}. The same model with minor modification applies to dissolution processes, however, the simulations shown here are only for surface deposition.

Case 6. Nucleation via first-order chemical reaction:

$$A_0 \xrightarrow{K_N} A_1$$

where A_0 is a precursor species and A_1 is the nucleus formed by the reaction, and K_N is the first-order constant for the nucleation reaction. The simulations are run with $K_N = 5 \times 10^{-6}$ s^{-1}, and an initial precursor concentration 10^5 m^{-3}, an initial nucleus concentration $C_0 = 3000$ m^{-3} and dimensionless size $v/v_0 = 1$.

Case 7. Gravitational settling with rate,

$$E(v) = E_0 \left(\frac{v}{v_0}\right)^{2/3}, \quad E_0 = 10^{-5}\ s^{-1} \quad (20)$$

with initial particle concentration $C_0 = 10^{10}$ m^{-3}.

The simulation tracks the dimensionless particle mass, v/v_0, and in all cases the initial state is monodisperse with $v/v_0 = 1$.

Table 2
Computational details

Case	Parameter	Stepwise constant-V	Constant-N	Time-driven DSMC	MMC
1 (constant kernel)	N§	1000	1000	1000	1000
	a	–	–	0.01	0.01
	CPU (s)	18.07	45.15	5.55	13.01
2 (linear kernel)	N§	2000	2000	2000	2000
	a	–	–	0.005	0.005
	CPU (s)	23.52	71.67	41.30	208.79
3 (quadratic kernel)	N§	2000	2000	2000	2000
	a	–	–	0.01	0.01
	CPU (s)	14.81‡ (12.43†)	49.97† (54.18‡)	49.13	241.80
4 (breakage)	N§	3000	3000	3000	3000
	a	–	–	0.0002	0.0002
	CPU (s)	6.55	2.99	21.71	20.59
5 (surface growth)	N§	3000	3000	3000	3000
	a	–	–	0.01	0.001
	CPU (s)	101.28	104.68	47.39	578.01
6 (nucleation)	N§	3000	3000	3000	3000
	a	–	–	–	–
	CPU (s)	6.51	3.01	6.59	29.60
7 (settling)	N§	3000	3000	3000	3000
	a	–	–	0.00033	0.001
	CPU (s)	13.02	23.81	29.90	142.02

Memory allocation (all cases): $O(N)$

§For stepwise constant-V and time-driven DSMC, N refers to the initial number of particles in the simulation.

†Using acceptance/rejection method; ‡ Using inverse method; in all other cases, step-wise constant-V implements inverse method while constant-N implements acceptance/rejection.

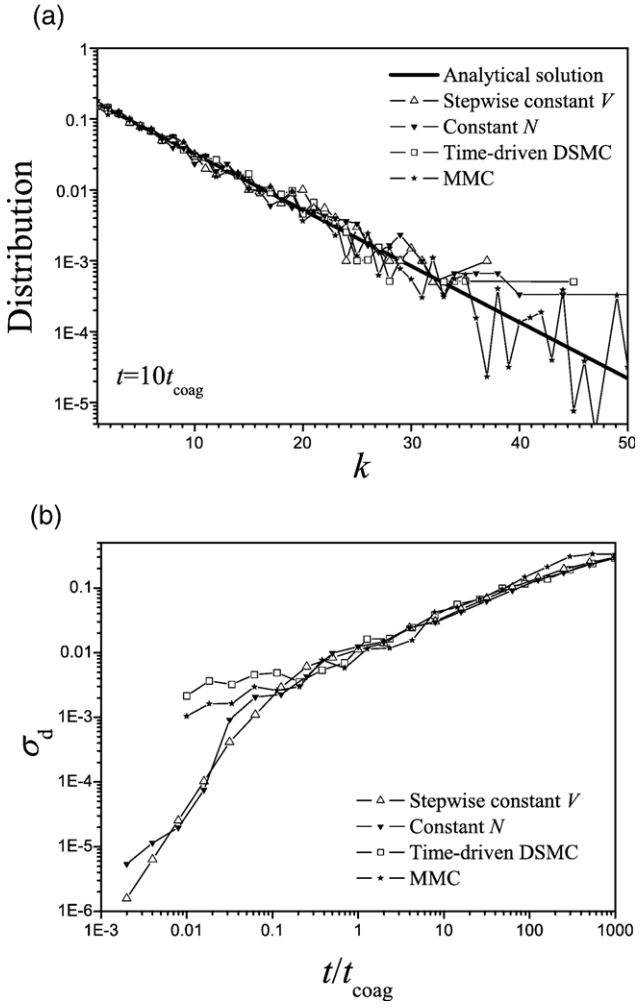

Fig. 1. Results for constant kernel (case 1): (a) size distributions; (b) error in size distributions.

For all test cases we compute the number and mass concentrations as a function of time, as well as the size distributions for cases 1–4 (in cases 6 and 7 the size distribution remains monodisperse and in case 5 nearly monodisperse). The results shown represent the average of three simulations with different seeds for the random number generator. Additional computational details are reported in Table 2. Unless stated otherwise, the stepwise constant-V method is implemented using the inverse method and the constant-N method using the acceptance/rejection method.

3.2. Coagulation (cases 1, 2, 3)

The three coagulation kernels examined here are the so-called classical kernels whose analytic solution is known [49]. Detailed results for the constant kernel are shown in Figs. 1–3 (case 1). The linear and quadratic kernels (cases 2 and 3) exhibit very similar behavior and are not shown. Fig. 1a shows the size distribution at $t=10t_{\mathrm{coag}}$, where $t_{\mathrm{coag}}=1/C_0\beta_0$. All methods track the size distribution well. In all cases the fluctuations of the computed distributions increase at the high-end of the distribution because of the smaller number of particles in this size range. Among the four methods, MMC exhibits the least error at the high-end of the size distribution. This is a result of the statistical weights, k_{wt}, which effectively increase the number of particles tracked by the MMC method.

To compare the relative performance on a quantitative basis, we compute the overall error in the size distribution, σ_{d}, as follows:

$$\sigma_{\mathrm{d}}=\left\{\frac{1}{K}\sum_{k=1}^{K}\frac{(n_k-n_k^{\mathrm{th}})^2}{n_{\mathrm{tot}}^2}\right\}^{1/2} \tag{21}$$

where n_k is the number of clusters containing k primary particles, n_k^{th} is the theoretical value, n_{tot} is the total number of particles in the simulation and K is the total number of particle masses in the simulation. Values of σ_{d} are averaged over three runs and the results are shown in Fig. 1b. Initially, the event-driven methods perform more accurately but for times longer than about $t/t_{\mathrm{coag}}\sim 1$ the error for all four methods practically collapses onto a single curve that slowly increases with time. In this regime, all methods yield nearly identical error.

Fig. 2a shows the evolution of the number distribution in the form of the ratio C/C_{theory}. The associated error, σ_{C}, shown in Fig. 2b, is calculated as the standard deviation of the fluctuations seen in Fig. 2a, averaged over three independent

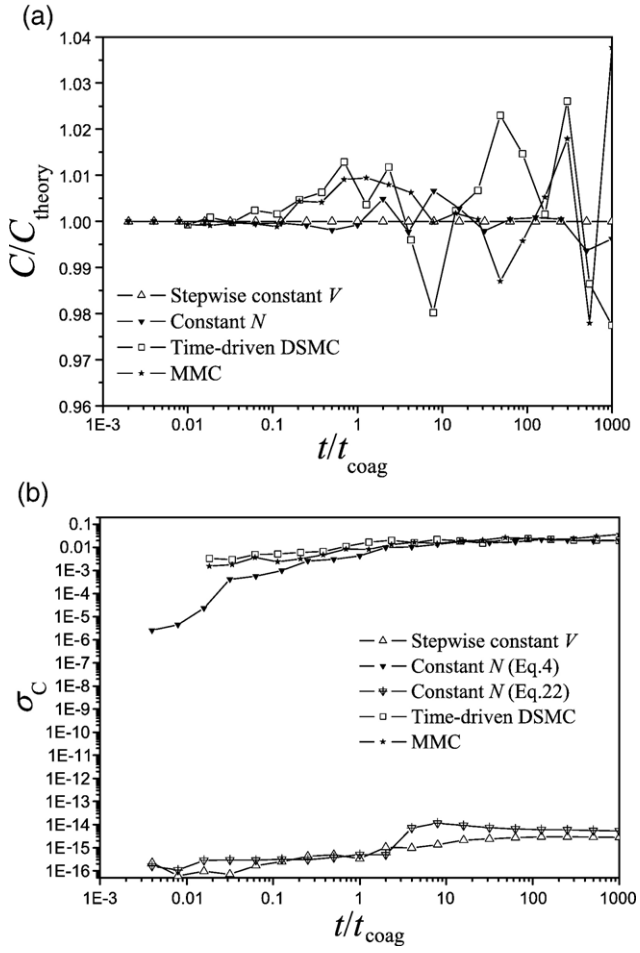

Fig. 2. Results for constant kernel (case 1): (a) number concentration; (b) error in number concentration.

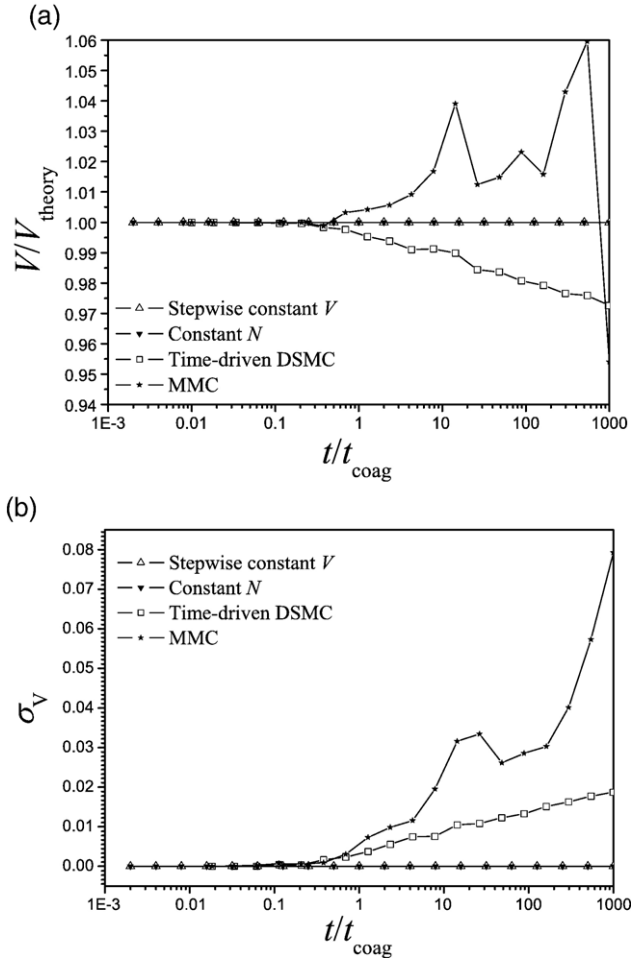

Fig. 3. Results for constant kernel (case 1): (a) mass concentration; (b) error in mass concentration.

runs. A similar analysis of the mass concentration is shown in Fig. 3. Stepwise constant-V is in exact agreement with the mass concentration, and gives the smallest error in the number concentration. The constant-N method is exact for the mass concentration but shows a larger error in the number concentration. The two time-driven methods produce error with respect to both the number and mass concentrations. This varied behavior reflects the different approaches by which each method advances time. In time-driven methods the time step is specified by the user. As with any standard integration technique, the accuracy improves if the integration step is reduced, but this improvement comes at the expense of computational time. Event-driven methods, on the other hand, do not specify the time step: instead, this step is given by the mean time that elapses between events. In event-driven methods that regulate the particle number continuously, there is added flexibility to fine-tune the calculation of the time step. For example, the time increment in the constant-N method can be improved if it is calculated as suggested in Lee and Matsoukas [25]:

$$\Delta t' = \frac{v_k}{\bar{v}} \cdot \frac{C}{N} \frac{1}{\sum_i R_i} \tag{22}$$

where v_k is the particle mass that is chosen to fill the vacancy in the simulation box after a coagulation event. This expression, which represents a variation on Eq. (4) is indeed more accurate, as Fig. 2b shows. Such detailed considerations are, however, beyond the scope of this study and for this reason we will continue to use the simpler Eq. (4) in the implementation of the constant-N method.

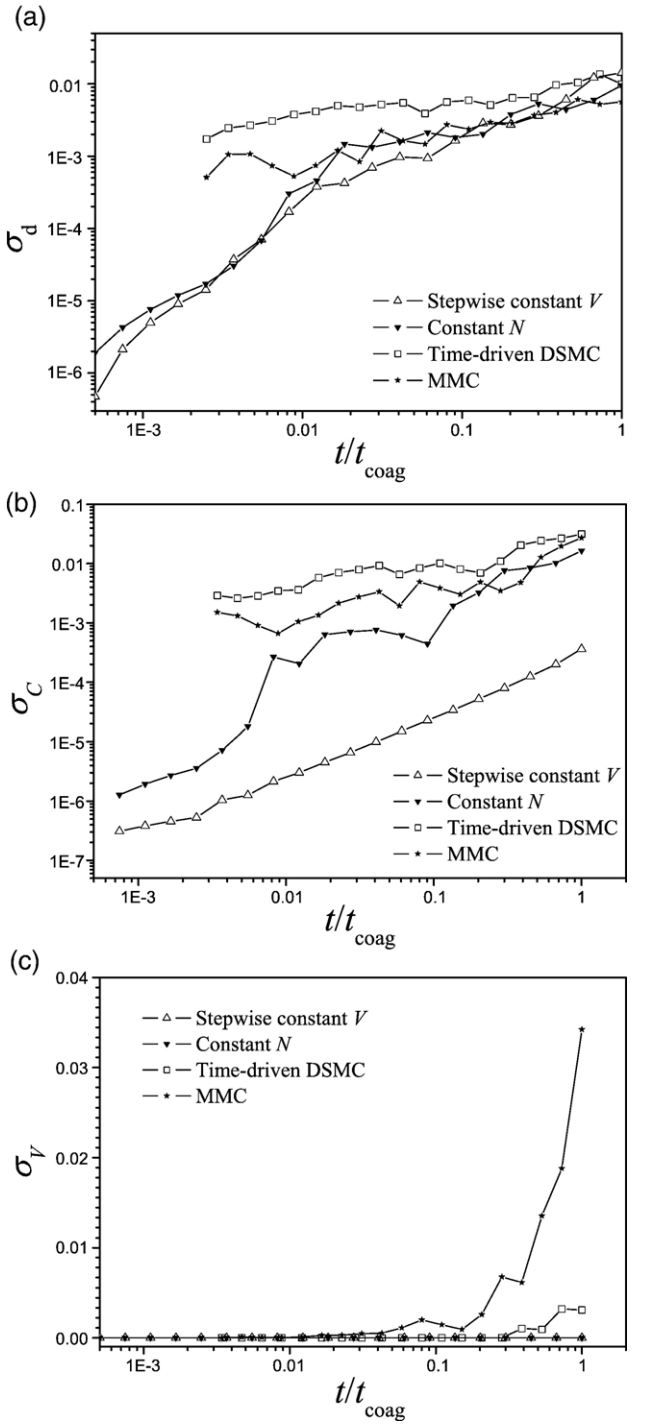

Fig. 4. Results for linear kernel (case 2): (a) linear kernel, error in distribution; (b) linear kernel, error in number concentration; (c) linear kernel, error in mass concentration.

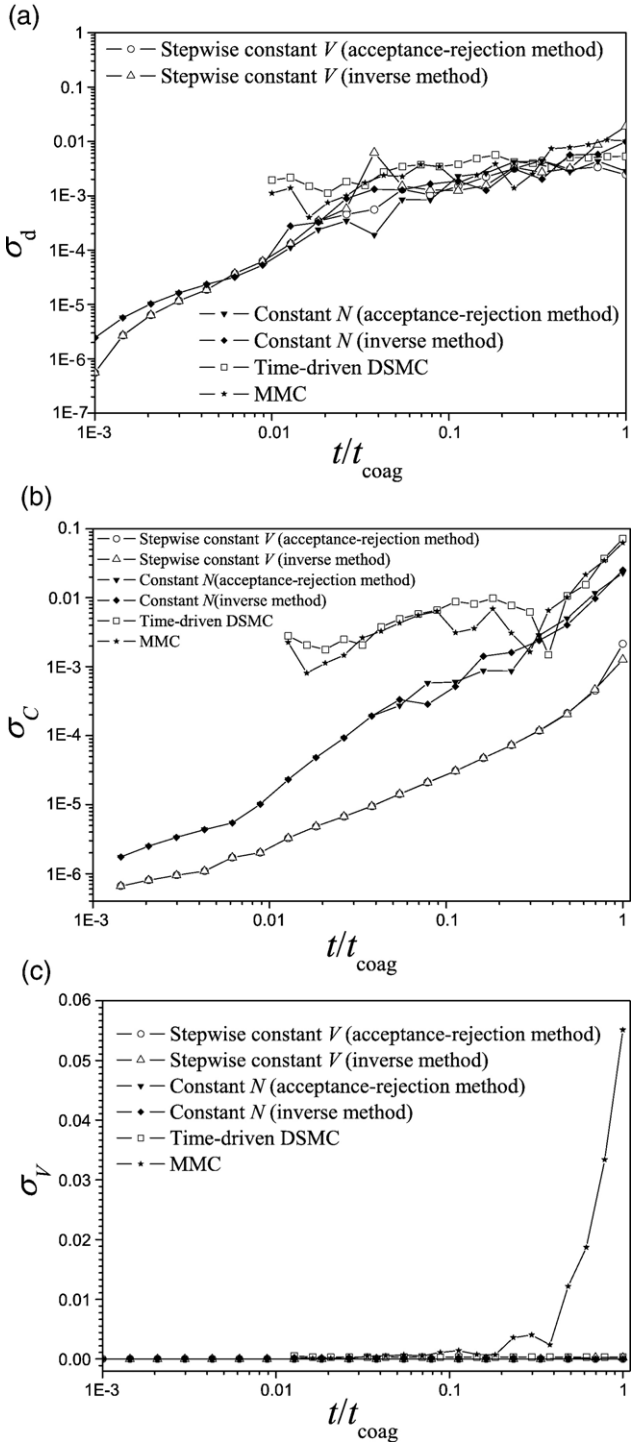

Fig. 5. Results for quadratic kernel (case 3): (a) quadratic kernel, error in distribution; (b) quadratic kernel, error in number concentration; (c) quadratic kernel, error in mass concentration.

Fig. 4 shows the errors in the distribution, number concentration and mass concentration for coagulation with the linear kernel. Similar graphs for the quadratic kernel are shown in Fig. 5. Qualitatively, the behavior of all kernels is the same: the error in the size distribution appears to converge for all four methods, while the error in the concentration (number and mass) is larger for the time-driven methods. We have further used the quadratic kernel as a test case for the relative performance of the acceptance/rejection and the inverse methods. For this purpose, the two event-driven algorithms, constant-N and stepwise constant-V, were tested with both acceptance/rejection and inverse method and the results are shown in Fig. 5. As we see, the error is not affected by the methodology that is chosen to select events. What is affected, however, is the computational time (see Table 2). In the case of the quadratic kernel, the acceptance/rejection method remains somewhat faster both in stepwise constant-V MC (12.43 s) and constant-N MC (49.97 s) compared to the inverse method (14.81 s in stepwise constant-V MC, and 54.18 s in constant-N MC).

3.3. Breakage (case 4)

This breakage model produces 12 equal-size fragments and results in sharp increase of the number of particles with time and in the formation of a wide size distributions. The analytic solution for this model is reported in [50]. The size distribution is shown in Fig. 6 at $t=0.5t_{brk}$ and $t=50t_{brk}$, where $t_{brk}=1/S_0$. Because all fragments of a parent particle are of equal size, the distribution is sparse as it contains particles only at masses that are powers of 1/12. The distribution is predicted very well by all methods. The corresponding error, is shown in Fig. 6b, and, as in coagulation, we

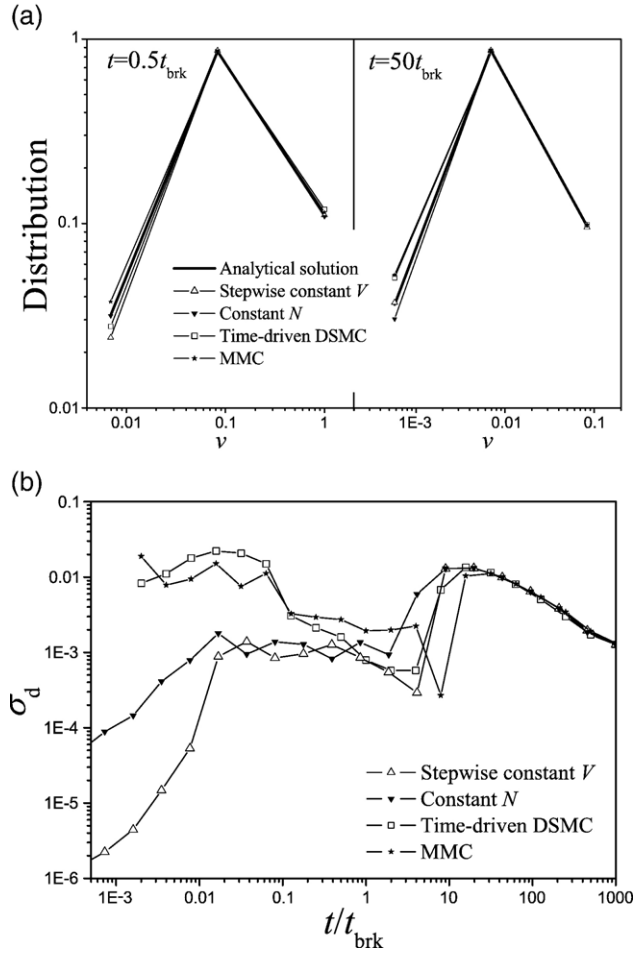

Fig. 6. Results for breakage (case 4): (a) size distributions; (b) error in size distributions.

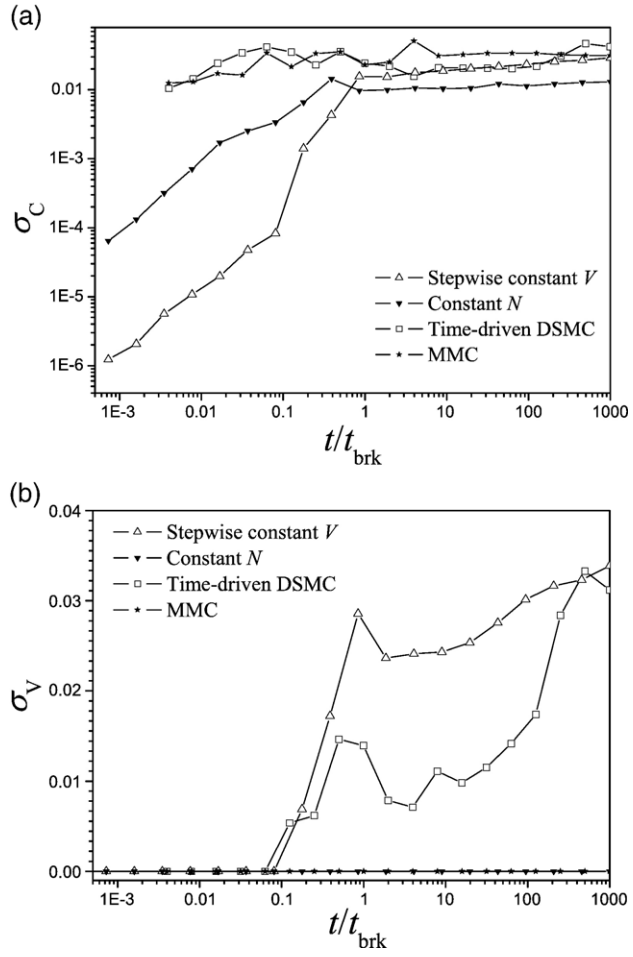

Fig. 7. Results for breakage (case 4): (a) error in number concentration; (b) error in mass concentration.

notice that all four methods converge to remarkably similar error after $t \approx 10_{brk}$. The number concentration is predicted very well by the event-driven methods and with somewhat larger error by the time-driven methods (Fig. 7a). We further notice that constant-N and MMC conserve the mass of the particles with great accuracy, while stepwise constant-V and time-driven DSMC exhibit larger

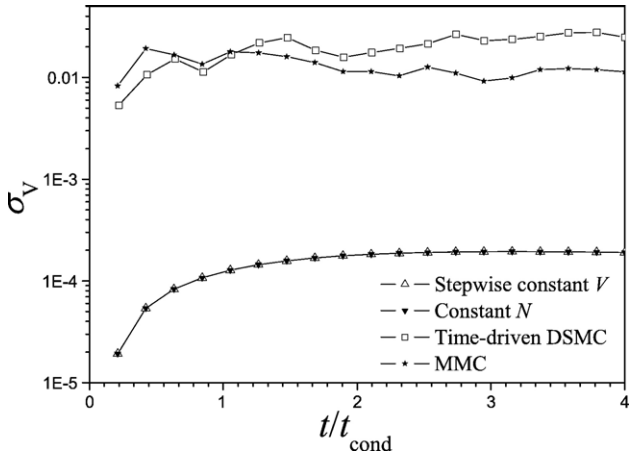

Fig. 8. Results for surface growth (case 5): error in mass concentration.

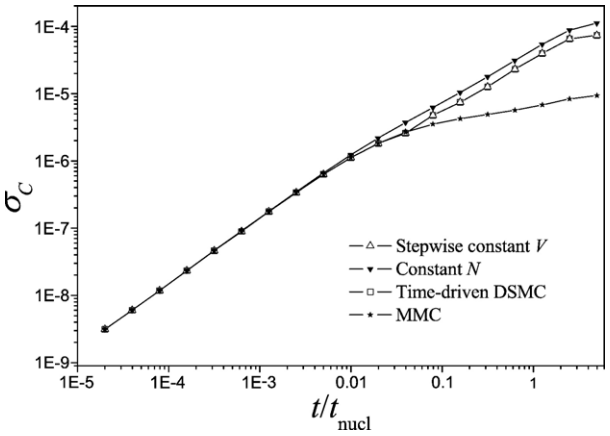

Fig. 9. Results for nucleation (case 6): error in number concentration.

errors, which, however, remain smaller than 4% (Fig. 7b). This discrepancy originates from the peculiarities of halving the population, specifically, from the fact that the number of particles in the simulation box cannot be exactly doubled when breakage in twelve pieces is considered. As a result, several particles must be added or discarded randomly to restore the sample size after halving. This problem can be avoided if N is divisible by $m-1$, where m is the number of fragments after each breakage.

3.4. Surface growth (case 5)

In this model, a chemical precursor, of size v_S and with initial concentration C_{S0}, deposits on the surface of particles with linear growth law. The concentration of particles is C_0 and the initial particle size is $v_0 = v_S$. The analytical solution for the number and mass concentrations is

$$C = C_0, \quad V = C_0 v_S e^{t/t_S}, \quad t_S = 1/C_0 K_S(v_S) \tag{23}$$

The size distribution for this model is nearly monodisperse and the number concentration remains, by model assumption, constant. Therefore, results are shown only for the mass concentration, C (see Fig. 8). All methods here have very high precision for linear condensation case. This is largely a

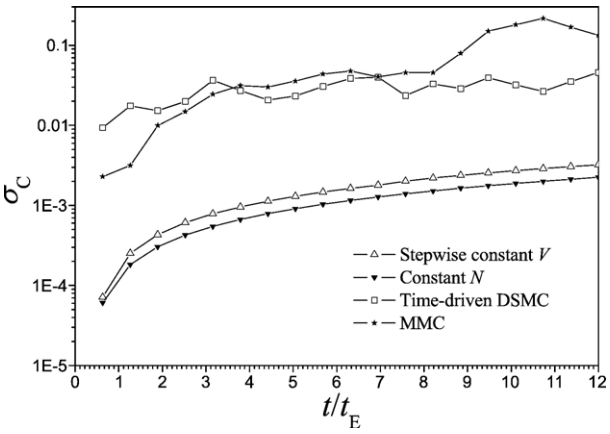

Fig. 10. Results for settling (case 7): error in number concentration.

consequence of the fact that the number of particles remains constant, thus no regulation of the sample size is required. The two event-driven methods are equivalent in this case and lead to identical results. The two time-driven methods are equivalent if every particle in the MMC simulation is tracked (i.e. if $k_{wt}=1$ for all particles). The small differences between the time-driven methods are due to the different value of a used (0.001 in MMC, 0.01 in time-driven DSMC).

3.5. Nucleation (case 6)

In this model we consider the formation of new particles fueled by a first-order chemical reaction, in the absence of any other growth mechanism. The number concentration, C, and the mass concentration, V, are given by

$$C = C_0 + A_0(1-e^{-t/t_{nucl}}) \tag{24}$$

$$V = v_{nucl}C \tag{25}$$

where C_0, v_{nucl}, are the number concentration and size of nuclei present at time zero, A_0 is the precursor concentration at time zero, and $t_{nucl}=1/K_N$. Since particle number and volume concentration differ only by a multiplicative constant, results are only shown for the error in the number concentration, σ_C (Fig. 9). All four MC's describe the dynamic evolution of nucleation very well and while the error increases with time, it remains below 0.01%.

3.6. Gravitational settling (case 7)

In this model, particles are assumed to exit the reactor volume with a rate that is proportional to the 2/3 power of the particle mass. The number concentration, C, and mass concentration, V, are given by

$$C = C_0 e^{-t/t_E} \tag{26}$$

$$V = v_0 C \tag{27}$$

where v_0 is the particle size, $t_E=1/E_0$, and E_0 is the rate constant for settling. In this model the particle size distribution remains monodisperse and the mass distribution is directly proportional to the number distribution. Fig. 10 shows the error in the number concentration. The result is very similar to that seen in case 5 (surface growth) with the event-driven methods showing much less error than the time-driven methods.

4. Discussion

The effect of the number of particles on accuracy has been previously studied for both constant-N [24] and stepwise constant-V [31,32] and as in all Monte Carlo methods in general, it was found that increasing the number of simulation particles increases the accuracy of the calculation. To provide a common basis for comparison, we have conducted the present simulations with comparable numbers of particles. Given the peculiarities of the algorithms, it is not possible to keep the number of particles exactly the same in all methods; in stepwise constant-V and in time-driven DSMC, for example, the number of simulation particles oscillates between N and $2N$ (or $N/2$) and is not constant. For these two methods, the reported number of particles (see Table 2) is that at the beginning of the simulation. Perhaps the most important conclusion of this study is that the error in the size distribution is very similar for all four methods, when comparable numbers of simulation particles are used. This conclusion stands both in coagulation and in breakage problems.

The second observation is that performance overall depends on whether the method is event- or time-driven. The two event-driven methods, constant-N and stepwise constant-V are very similar in concept and perform at nearly identical levels of accuracy. In the constant-N method, the size of the simulation box is adjusted after each and every event so as to contain N particles. The stepwise method begins with N_0 particles and the simulation box is readjusted when the number of particles reaches $2N_0$ or $N_0/2$, as the case may be. The artificial regulation of the simulation box introduces some noise in the simulation. In the constant-N method, this happens at the end of each event, whenever a particle is added or removed. In the stepwise constant-V method it only happens with mechanisms that increase the number of particles because the halving of the simulation box does not necessarily decrease all size classes by a factor of 2. With respect to mass concentration, constant-N and stepwise constant-V perform with high accuracy, both with mechanisms that conserve the mass of the particle population (coagulation, breakage) and with those that do not (surface growth, nucleation, settling). With respect to the number concentration, the relative performance depends on the particular problem (stepwise constant-V performs better in coagulation, but constant-N performs better in breakage) but such differences can be minimized if refinements such as Eq. (22) are used.

Time-driven methodologies calculate the size distribution with comparable accuracy as the event-driven methods. These methods, however, tend to larger error in the number and mass distribution, especially at longer simulation times. The main source for this error is the fact that dynamic events within the time step Δt may depend on each other and are not uncoupled. This error can be reduced by decreasing the multiplicative constant α but this also leads to longer computational times. It is worth noting that the MMC method is capable of tracking the size distribution to larger sizes compared to all other methods. This is attributed to the weight factors, k_{wt}, which effectively increase the number of particles beyond the nominal number in the simulation box.

The computational costs are summarized in Table 2, and all of simulation are taken in the same desktop PC equipped with Athlon XP2500+, 512M, Visual Fortran 6.0 and Windows XP professional. The CPU times reported should only be compared within the same case because the simulation time varies among cases. The CPU time depends on the number of simulation particles and for the time-driven methods on the parameter α as well. Since the number of simulation particles is not the same in

all methods, direct comparisons are not entirely appropriate. In stepwise constant-V and time-driven DSMC the number of simulation particles varies with time: in coagulation it ranges from N_0 initially to $N_0/2$ but in breakage from N_0 to $2N_0$. As a result these methods tend to be faster in coagulation but slower in breakage when compared to their counterparts. For these reasons the reported CPU times should be understood as qualitative indicators of the required computational effort. It can be seen that overall, event-driven methods are faster than time-driven methods.

The algorithms studied in this paper represent four Monte Carlo variants that are in common use for solving population balances. All of the methods implement some method of controlling the number of particles within predetermined bounds and thus are capable of tracking population balances over arbitrarily long simulation times. Event-driven methods retain the straightforward logic of Monte Carlo and lead to equally straightforward numerical code. An important feature of these methods is that the time increment is not fixed as it is given by the inverse of all rates. This is not a concern if the simulation is a stand-alone computation. If the purpose is to simulate a particulate population within a larger unit operation, event-driven methods are at a disadvantage because process simulators work with standard integrators that are time-driven. Time-driven MC is more suitable in this case and could lead to large scale simulations that would not only capture particulate mechanisms but also the space evolution of PSD, boundary conditions and even gas-particle dynamics coupling with two-phase flow models.

5. Conclusions

Four MC methods, constant-N, stepwise constant-V, time-driven direct simulation, and multi-Monte Carlo simulation, were employed numerically to simulate the dynamic evolution in a variety of mechanisms that typically appear in particulate processes. The methods have been compared with respect to accuracy in the distribution, accuracy in the number and mass concentration of particles, as well as with respect to CPU requirements. For the first time, the accuracy of MC methods has been quantified on basis of standard deviations in calculation of properties of particle size distribution. This approach can be used for accuracy analysis of new and modified MC methods. With respect to the size distribution, there is remarkable similarity in accuracy among all four methods, despite the fact that each method regulates differently the number of particles in the simulation. Thus we conclude that the error in the calculated size distribution is primarily controlled by the number of simulation particles. The larger variability seen with respect to the time evolution of the number or mass concentration depends mainly on the details of how the time increment is implemented rather than the size of the simulation box. With regards to the computational time, event-driven methods have an advantage over time-driven methods because an event is by design guaranteed to happen in each step, thus advancing the simulation further in time. The choice between step-wise constant-V and constant-N methods may be made on the basis of expected behavior of the particle number concentration. If it is expected that particle number concentration increases during the process, constant-N method should perform better than stepwise constant-V method. The situation is reversed if the number concentration is expected to decrease — the stepwise constant-V method would be faster and more accurate than constant-N method. Time-driven algorithms are more suitable in cases where the population balance equation is to be solved within a larger process simulator that performs explicit integrations in time. Overall, very good accuracy can be achieved using reasonably small numbers of simulation particles, $O(10^3)$, requiring computational times of the order 10^2-10^3 s in typical desktop systems.

Notation

C	Number concentration, (m^{-3})
E	Rate of settling, (s^{-1})
C_{theory}	Number concentration in exact solution, (m^{-3})
$K_S(v)$	Rate of deposition onto particles of size v (m^3 s^{-1})
k_{wt},i	Statistical weight of particle i
N_0	Initial number of simulation particles
$n(v)$	Size distribution (m^{-6})
n_k	Number distribution of simulation particles of size $v=kv_0$
P	Probability
R_l	Specific rate of event l ($m^{-3}s^{-1}$)
$S(v)$	Breakage rate of size v (s^{-1})
S_0	Pre-factor of breakage rate of size v (s^{-1})
t	Time (s)
t_{coag}	Characteristic coagulation time (s)
$t_{coag,i}$	Coagulation time of particle i (s)
t_{brk}	Characteristic breakup time (s)
t_S	Characteristic surface growth time (s)
t_{nucl}	Characteristic nucleation time (s)
t_E	Characteristic settling time
V	Mass concentration of particles (kg m^{-3})
V_{theory}	Mass concentration − exact solution (kg m^{-3})
v	Particle mass (size) (m^3)
$\overline{v}$	Average particle mass (m^3)
v_0	Particle mass at time 0 (m^3)
v_k	Mass of particle added to or removed from simulation box (m^3)
v_S	Volume of the condensing species (m^3)
V_s	Volume of the simulated system (m^3)
v_{nucl}	Size of the nucleus (m^3)

Greek letters

α	Parameter controlling the time increment in time-driven MC
$\beta(v_i,v_j)$	Coagulation kernel between sizes v_i and v_j, m^3/s
β_0	Pre-factor of coagulation kernel, m^3/s
$\Gamma(v\|u)$	Fragments with size in (v, $v+dv$)produced from size u; (m^{-3})
δv_{event}	Change in mass due to event
Δt	Time increment (s)
σ_d	Error in size distribution
σ_C	Error in number concentration
σ_V	Error in mass concentration

Acknowledgements

H. Zhao wishes to thank "National Key Basic Research and Development Program 2006CB200304 and 2002CB211602" and "the National Natural Science Foundation of China under grant number 90410017 and 20606015" for funds.

References

[1] W. Seames, An initial study of the fine fragmentation fly ash particle mode generated during pulverized coal combustion, Fuel Process. Technol. 81 (2003) 109–125.
[2] F. Lockwood, S. Yousif, A model for the particulate matter enrichment with toxic metals in solid fuel flames, Fuel Process. Technol. 65– 66 (2002) 439–457.
[3] D. Kim, M. Gautam, D. Gera, Parametric studies on the formation of diesel particulate matter via nucleation and coagulation modes, J. Aerosol Sci. 33 (2002) 1609–1621.
[4] A. Sandu, A Newton Cotes quadrature approach for solving the aerosol coagulation equation, Atmos. Environ. 36 (2002) 583–589.
[5] R. Fan, D.L. Marchisio, R.O. Fox, Application of the direct quadrature method of moments to polydisperse gas–solid fluidized beds, Powder Technol. 139 (1) (2004) 7–20.
[6] D.L. Wright, R. McGraw, D.E. Rosner, Bivariate extension of the quadrature method of moments for modeling simultaneous coagulation and sintering of particle populations, J. Colloid Interface Sci. 236 (2) (2001) 242–251.
[7] R. McGraw, Description of aerosol dynamics by the quadrature method of moments, Aerosol Sci. Technol. 27 (2) (1997) 255–265.
[8] A. Zucca, D.L. Marchisio, A.A. Barresi, R.O. Fox, Implementation of the population balance equation in CFD codes for modelling soot formation in turbulent flames, Chem. Eng. Sci. 61 (1) (2006) 87–95.
[9] D.L. Marchisio, D.R. Vigil, R.O. Fox, Implementation of the quadrature method of moments in CFD codes for aggregation-breakage problems, Chem. Eng. Sci. 58 (15) (2003) 3337–3351.
[10] C.A. Dorao, H.A. Jakobsen, Numerical calculation of the moments of the population balance equation, J. Comput. Appl. Math. 196 (2) (2006) 619–633.
[11] V. Alopaeus, M. Laakkonen, J. Aittamaa, Numerical solution of moment-transformed population balance equation with fixed quadrature points, Chem. Eng. Sci. 61 (2006) 4919–4929.
[12] D.L. Marchisio, R.D. Vigil, R.O. Fox, Quadrature method of moments for aggregation-breakage processes, J. Colloid Interface Sci. 258 (2) (2003) 322–334.
[13] D.L. Marchisio, R.O. Fox, Solution of population balance equations using the direct quadrature method of moments, J. Aerosol Sci. 36 (1) (2005) 43–73.
[14] R.B. Diemer, J.H. Olson, A moment methodology for coagulation and breakage problems: part 2-moment models and distribution reconstruction, Chem. Eng. Sci. 57 (12) (2002) 2211–2228.
[15] R.B. Diemer, J.H. Olson, A moment methodology for coagulation and breakage problems: part 1-analytical solution of the steady-state population balance, Chem. Eng. Sci. 57 (12) (2002) 2193–2209.
[16] F. Gelbard, J.H. Seinfeld, Simulation of multicomponent aerosol dynamics, J. Colloid Interface Sci. 78 (2) (1980) 485–501.
[17] J. Landgrebe, S. Pratsinis, Gas-phase manufacture of particulate: interplay of chemical reaction and aerosol coagulation in the free-molecular regime, Ind. Eng. Chem. Res. 28 (1989) 1474–1481.
[18] J. Wu, R. Flagan, A discrete-sectional solution to the aerosol dynamic equation, J. Colloid Interface Sci. 123 (1988) 339–352.
[19] J.D. Landgrebe, S.E. Pratsinis, A discrete-sectional model for particulate production by gas-phase chemical reaction and aerosol coagulation in the free-molecular regime, J. Colloid Interface Sci. 139 (1) (1990) 63–86.
[20] D.T. Gillespie, The stochastic coalescence model for cloud droplet growth, J. Atmos. Sci. 29 (1972) 1496–1510.
[21] B.H. Shah, D. Ramkrishna, J.D. Borwanker, Simulation of particulate systems using the concept of the interval of quiescence, AIChE J. 23 (1977) 897–904.
[22] A.L. Garcia, C. van den Broeck, M. Aertsens, R. Serneels, A Monte Carlo simulation of coagulation, Physica, A Stat. Theor. Phys. 143 (3) (1987) 535–546.
[23] K. Liffman, A direct simulation Monte–Carlo method for cluster coagulation, J. Comput. Phys. 100 (1) (1992) 116–127.
[24] M. Smith, T. Matsoukas, Constant-number Monte Carlo simulation of population balances, Chem. Eng. Sci. 53 (9) (1998) 1777–1786.
[25] K. Lee, T. Matsoukas, Simultaneous coagulation and break-up using constant-*N* Monte Carlo, Powder Technol. 110 (2000) 82–89.
[26] Y. Lin, K. Lee, T. Matsoukas, Solution of the population balance equation using constant-number Monte Carlo, Chem. Eng. Sci. 57 (2002) 2241–2252.
[27] A. Kolodko, S.K., W. Wagner, A stochastic method for solving Smoluchovski's coagulation equation, Math. Comput. Simul. 49 (1999) 57–79.
[28] J. Laurenzi, J.D. Bartels, S.L. Diamond, A general algorithm for exact simulation of multicomponent aggregation processes, J. Comput. Phys. 177 (2002) 418–449.
[29] M. Goodson, M. Kraft, An efficient stochastic algorithm for simulating nano-particle dynamics, J. Comput. Phys. 183 (2002) 210–232.
[30] A. Vikhansky, M. Kraft, A Monte Carlo methods for identification and sensitivity analysis of coagulation processes, J. Comput. Phys. 200 (2004) 50–59.
[31] F.E. Kruis, A. Maisels, H. Fissan, Direct simulation Monte Carlo method for particle coagulation and aggregation, AIChE J. 46 (9) (2000) 1735–1742.
[32] A. Maisels, F. Einar Kruis, H. Fissan, Direct simulation Monte Carlo for simultaneous nucleation, coagulation, and surface growth in dispersed systems, Chem. Eng. Sci. 59 (11) (2004) 2231–2239.
[33] H. Zhao, C. Zheng, Monte Carlo solution of wet scavenging of aerosols by precipitation, Atmos. Environ. 40 (8) (2006) 1510–1525.
[34] H. Zhao, C. Zheng, M. Xu, Multi-Monte Carlo approach for general dynamic equation considering simultaneous particle coagulation and breakage, Powder Technol. 154 (2–3) (2005) 164–178.
[35] H. Zhao, C. Zheng, M. Xu, Multi-Monte Carlo method for coagulation and condensation/evaporation in dispersed systems, J. Colloid Interface Sci. 286 (1) (2005) 195–208.
[36] H. Zhao, C. Zheng, M. Xu, Multi-Monte Carlo method general dynamic equation considering particle coagulation, Appl. Math. Mech. 26 (7) (2005) 953–962.
[37] T. Matsoukas, S.K. Friedlander, Dynamics of aerosol agglomerate formation, J. Colloid Interface Sci. 146 (1991) 495–506.
[38] D.T. Gillespie, An exact method for numerically simulating the stochastic coalescence process in a cloud, J. Atmos. Sci. 32 (1975) 1977–1989.
[39] P. Tandon, D.E. Rosner, Monte Carlo simulation of particle aggregation and simultaneous restructuring, J. Colloid Interface Sci. 213 (1999) 273–286.
[40] D.E. Rosner, S. Yu, Monte Carlo simulation of aerosol aggregation and simultaneous spheroidization, AIChE J. 47 (3) (2001) 545–561.
[41] D.E. Rosner, R. McGraw, P. Tandon, Multivariate population balances via moment and Monte Carlo simulation methods: an important sol reaction engineering bivariate example and mixed moments for the estimation of deposition, scavenging, and optical properties for populations of nonspherical suspended particles, Ind. Eng. Chem. Res. 42 (2003) 2699–2711.
[42] Y. Efendiev, M. Zachariah, Hybrid Monte Carlo method for simulation of two-component aerosol coagulation and phase segregation, J. Colloid Interface Sci. 249 (2002) 30–43.
[43] D.T. Gillespie, A general method for numerically simulating the stochastic time evolution of coupled chemical reactions, J. Comput. Phys. 22 (1976) 403–434.
[44] J.R.P. Gooch, M.J. Hounslow, Monte Carlo simulation of size-enlargement mechanisms in crystallization, AIChE J. 42 (7) (1996) 1864–1874.
[45] A. Maisels, F.E. Kruis, H. Fissan, Coagulation in bipolar aerosol chargers, J. Aerosol Sci. 35 (2004) 1333–1345.
[46] M. Lattuada, H. Wu, M. Morbidelli, A simple model for the structure of fractal aggregates, J. Colloid Interface Sci. 268 (2003) 106–120.

[47] E. Hollander, J.J. Derksen, O.S.L. Bruinsma, H.E.A. van den Akker, G.M. van Rosmalen, A numerical study on the coupling of hydrodynamics and orthokinetic agglomeration, Chem. Eng. Sci. 56 (2001) 2531–2541.
[48] T. Matsoukas, K. Lee, T. Kim, Mixing of components in two-component aggregation, AIChE J. 52 (9) (2006) 3088–3099.
[49] F. Leyvraz, Scaling theory and exactly solved models in the kinetics of irreversible aggregation, Phys. Rep. 383 (2–3) (2003) 95–212.
[50] M. Kostoglou, A.J. Karabelas, An assessment of low-order methods for solving the breakage equation, Powder Technol. 127 (2002) 116–127.